

5

Mitigation strategy for the drill-string experimental set-up

Vibrations, in general, cause great concerns in industry. Owing to the massive amount of money in oil operations, the avoidance of vibrations is almost imperative in order to prevent the increase of cost and time. However, as addressed in Chapters 1 and 2, the torsional vibrations are present in almost all oil wells due to the complex phenomena involved. Therewith, there is a big academic and industrial effort to a better understanding of the drilling system dynamics, proposing control and mitigation strategies of vibration to this kind of system, as one may also see in [26, 29, 47, 68, 89, 102, 115–118].

So far in this work, the experimental apparatus was presented in Chapter 3 as a drill-string like system in reduced scale with the goal to study dry friction-induced torsional vibrations in its severe stage: the stick-slip phenomenon. Following, the Chapter 4 consisted of the mathematical description as well as the stability analysis. The latter provided useful informations about locally stable solutions, including the coexistence of equilibrium and periodic solutions which are used in this chapter.

In this chapter, the achieved results are presented. The strategies are proposed in order to mitigate torsional vibration. For all numerical and experimental results, the normal force N_1 is maintained at 10 or 20 N. For the energy results, N_1 is kept 10 N. For other values of N_1 , the analyses are the same. Firstly, the numerical results of the mathematical model is presented in Section 5.1: the basins of attraction are performed in order to illustrate regions with and without torsional vibrations. Therefore, a mitigation strategy is proposed and analyzed. Following, Section 5.2 contains the experimental results: a servo controller is used to the pin motion at R_2 . Also, an embedded motor is used to provide perturbations on R_1 . This chapter ends with a summarization of the results, in Section 5.3.

5.1

Numerical results

Nonlinear dynamical systems may hold more than one solution such as equilibrium points, limit cycles, chaos, and quasi-periodic solutions. Thereby, the solution converges to one of those solutions according to their stability

properties and the initial conditions [105–107, 110].

Analyzing Figure 4.12, one may observe the possibility of periodic and equilibrium solutions for $2.0 \leq \omega_{ref} \leq 2.9 \text{ rad/s}$. To check the possibility of solutions in this velocity range, the torsional vibration factor¹ was used [15, 68, 69] as expressed below

$$f_{TV} = \frac{\max(\dot{\theta}_1) - \min(\dot{\theta}_1)}{2\omega_{ref}}, \quad (5-1)$$

where $f_{TV} = 0$ means no torsional vibration prevails, $\dot{\theta}_1 = \omega_{ref}$ and the solution is an equilibrium point, otherwise $f_{TV} > 0$ means torsional oscillations and the system presents stable limit cycles. An easy-to-understand physical example for the torsional vibration factor f_{TV} given by Eq. (5-1) is that: supposing $f_{TV} = 1.5$, then the vibration amplitudes will be 3 times the nominal angular velocity ω_{ref} , *i.e.*, this factor provides a direct correlation of the vibration magnitudes with the imposed (nominal) angular velocity.

The basins of attraction are depicted in Figure 5.1. The initial conditions were

$$x_0 = \left[\delta_{12}, \delta_{23}, \dot{\theta}_1, \dot{\theta}_2, \dot{\theta}_3, i \right]^T = \left[\delta_{12}, 0.0, \dot{\theta}_1, \omega_{ref}, \omega_{ref}, 1.022 \right]^T. \quad (5-2)$$

Herein, the current $i = 1.022 \text{ A}$ is the necessary value for steady-state with no perturbation obtained via simulation (acquired numerically). Using Eq. (5-1), one may observe the mentioned bi-stable solutions: Figure 5.1(a) presents a small equilibrium region which may difficult the change between stable solutions and the amplitudes are 2.40 times the ω_{ref} , whereas Figure 5.1(b) presents a significant equilibrium region which may lead to an effortless change of solutions with maximum amplitude of 2.10 times the ω_{ref} .

Therewith, one may ascertain that the solution depends on the perturbation to which the system is subjected in this angular velocity range [119]. Therefore, the mitigation strategy consists in applying a resistive torque in R_2 in order to create an *acceptable* and *sufficient* perturbation to change the solution from the periodic branch to the equilibrium branch, *i.e.*, the system may pass from torsional vibration to no torsional vibration.

Equation (5-3) provides the main energies involved. The damping energy is very small compared to the others.

¹Some authors denote this factor as “stick-slip severity”, however the system may oscillate without stick-slip phenomenon.

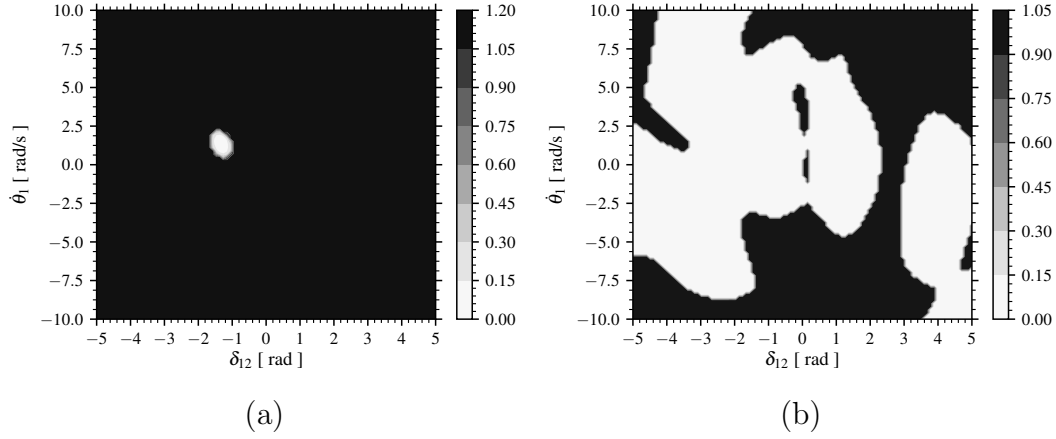


Figure 5.1: Basins of attraction for (a) $\omega_{ref} = 2.0 \text{ rad/s}$ and (b) $\omega_{ref} = 2.9 \text{ rad/s}$. The applied forces $N_1 = 10.0 \text{ N}$ and $T_{r_2} = 0.0 \text{ Nm}$. The white and black regions mean equilibria and periodic solutions, respectively.

$$\begin{aligned}
 E_{k_1} &= \frac{1}{2} J_1 (\omega_{ref} - \dot{\theta}_1)^2, & E_{k_2} &= \frac{1}{2} J_2 (\omega_{ref} - \dot{\theta}_2)^2, \\
 E_{p_1} &= \frac{1}{2} k_1 \delta_{12}^2, & E_{p_2} &= \frac{1}{2} k_2 \delta_{23}^2, \\
 W_{r_2} &= T_{r_2} \int_{t_1}^{t_2} (\omega_{ref} - \dot{\theta}_2) dt.
 \end{aligned} \tag{5-3}$$

It is worth to remark that the kinetic energies and work of the unperturbed system were subtracted in order to observe only the variation of these magnitudes, creating a relative kinetic energy. Also, keeping in mind that the system continues to rotate, the angle increases indefinitely and so the work of T_{r_2} is defined as that one which provide the variation between the ω_{ref} and $\dot{\theta}_2$.

Figure 5.2 illustrates the system energies (kinetic and potential) as functions of time in a stick-slip situation with $\omega_{ref} = 2.5 \text{ rad/s}$, *i.e.*, in the bi-stability angular velocity range. One may notice that the angular velocity at R_2 does not reach zero. However, Disc 1 (R_1) does perform stick-slip phenomenon remarked in Figure 5.2. After the $\dot{\theta}_1$ sticking, the Disc 1 accelerates, passing through the reference velocity ($E_{k_1} = 0$ at $t = 82.2 \text{ s}$). It reaches the maximum relative kinetic energy value (at $t = 82.8 \text{ s}$) and then it decelerates, passing again through the reference velocity ($E_{k_1} = 0$ at $t = 83.4 \text{ s}$) until sticking one more time.

5.1.1 First mitigation strategy

The first numerical approach as mitigation strategy may be written as follows

$$T_{r_2} = N_2 r_2 \mu_s \sin(k_f \delta_{12}). \tag{5-4}$$

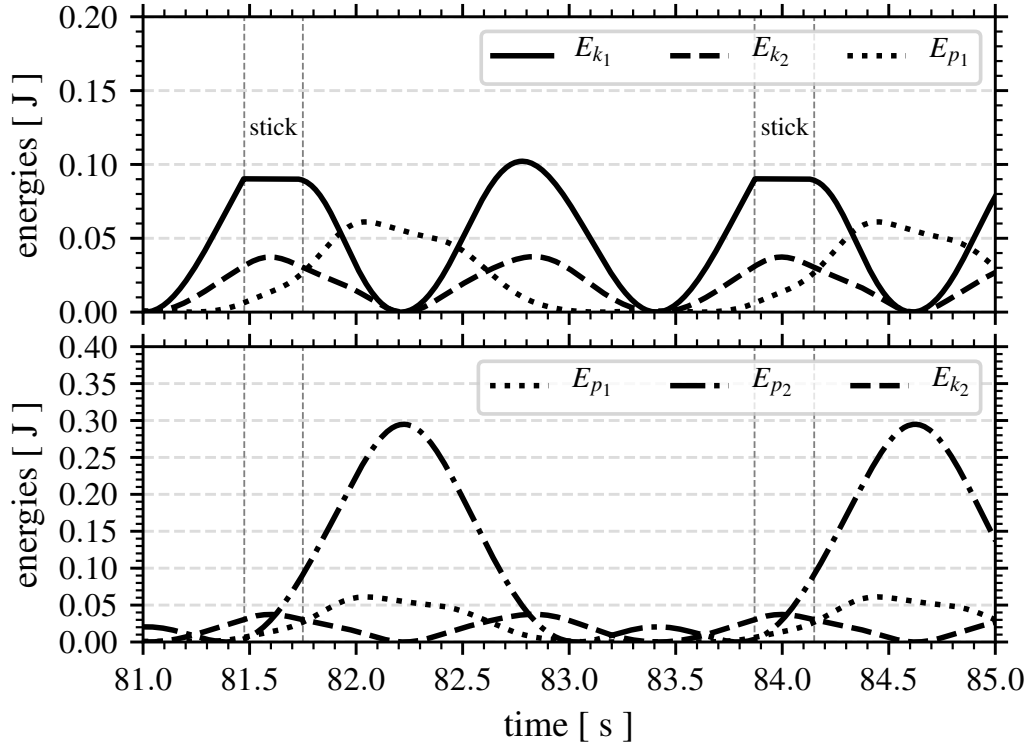


Figure 5.2: Relative kinetic and potential energies as function of time. $N_1 = 10.0$ N, $T_{r_2} = 0.0$ Nm, and $\omega_{ref} = 2.5$ rad/s.

Equation (5-4) is equivalent to applying impulsive torques depending on the magnitude of the phase, δ_{12} . The $k_f = \pi$ is an amplification factor which is kept constant.

Figure 5.3 shows the influence of Eq. (5-4) on the system during stick-slip phenomenon. One may observe that this first actuation proposal is not sufficient to mitigate torsional vibration with $N_2 = 1.0$ N because it does not provide enough perturbation to change the solution from periodic branch to equilibrium branch.

The increasing of N_2 to 5.0 N lead to a *sufficient* perturbation to change from periodic solution to an equilibrium solution, as shown in Figure 5.4: the strategy is applied in $t = 100$ s and it remains up to $t = 150$ s; thereafter, the system rotates with the same imposed angular velocity $\omega_{ref} = 2.5$ rad/s. However, this latter value of N_2 corresponds to 50% of N_1 . One may conclude that this normal force value is not *acceptable* for a mitigation strategy proposal since it would be large amount of energy to expend in the process. Figure 5.5 illustrates the involved energies of the system during this first mitigation strategy application with $N_2 = 5.0$ N: Figure 5.5(a) depicts the relative kinetic energies of disc R_1 and R_2 , and the work at R_2 , while Figure 5.5(b) illustrates the potential energies and the work at R_2 . The work provided by T_{r_2} with

the first strategy present the same order of magnitude (or larger) as the other involved energies.

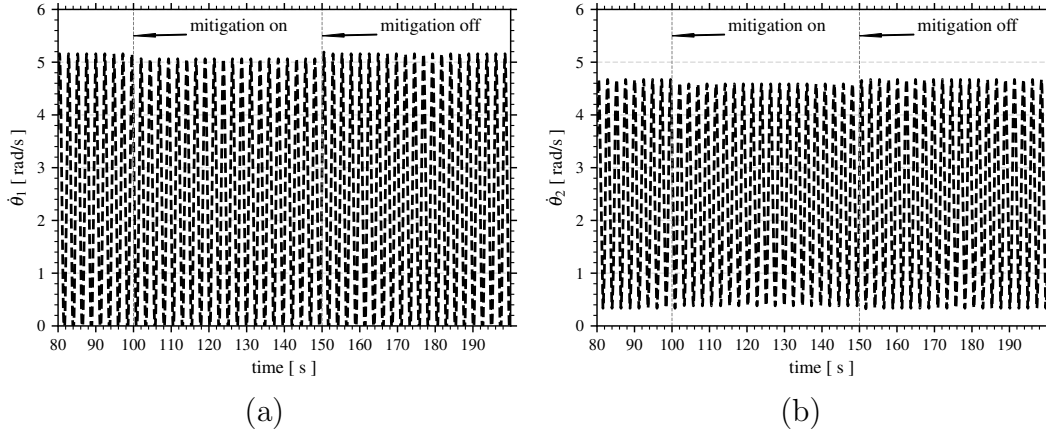


Figure 5.3: Influence of the mitigation strategy (a) on $\dot{\theta}_1$ and (b) on $\dot{\theta}_2$. $N_1 = 10.0$ N, $N_2 = 1.0$ N, and $\omega_{ref} = 2.5$ rad/s.

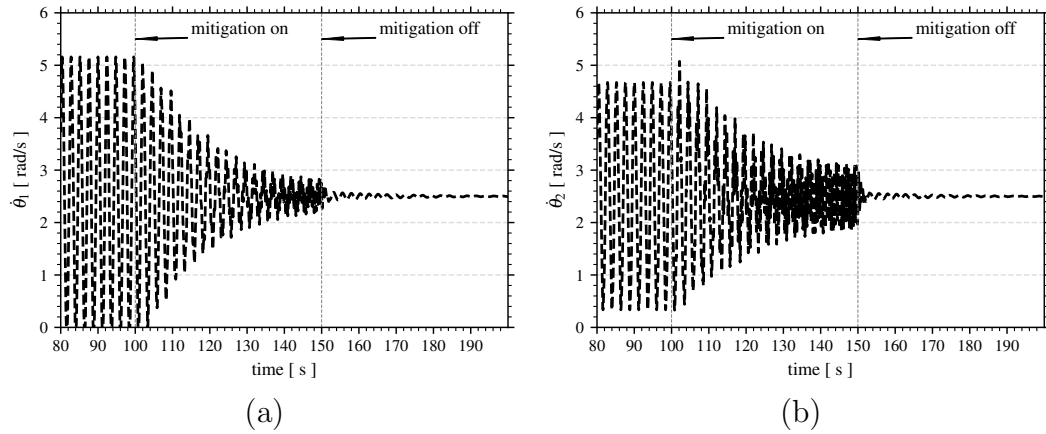


Figure 5.4: Influence of the mitigation strategy (a) on $\dot{\theta}_1$ and (b) on $\dot{\theta}_2$. $N_1 = 10.0$ N, $N_2 = 5.0$ N, and $\omega_{ref} = 2.5$ rad/s.

5.1.2

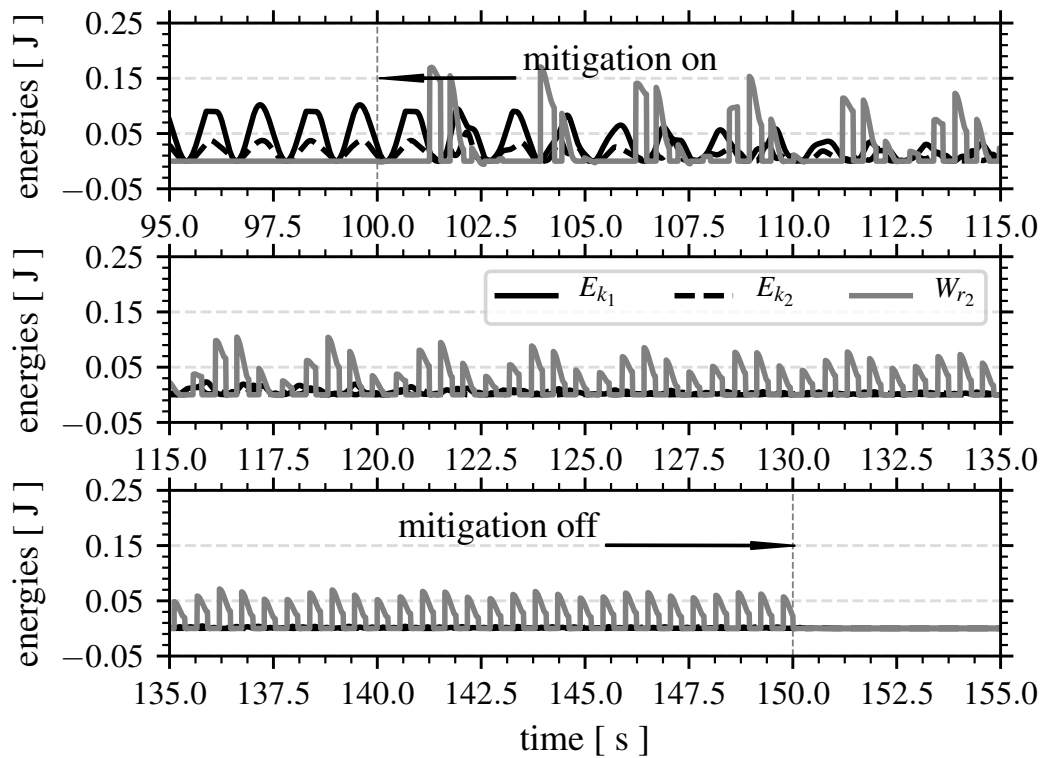
Second mitigation strategy

The resistive torque T_{r_2} may be rewritten as follows for the second approach

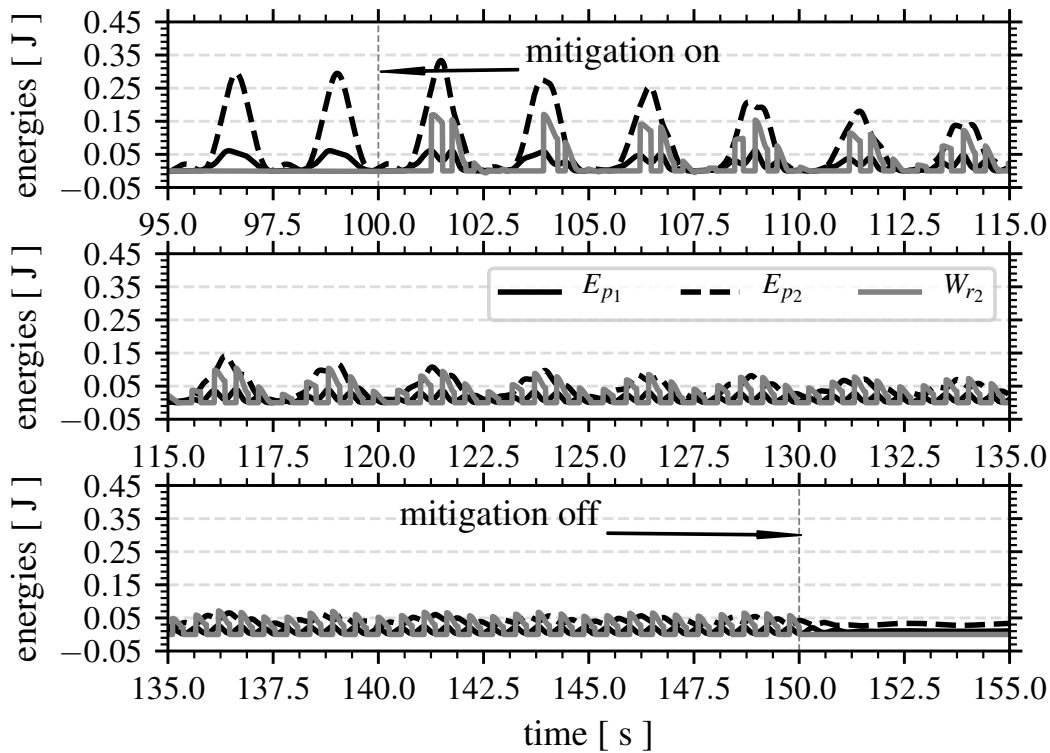
$$T_{r_2} = N_2 r_2 \mu_s \begin{cases} \sin(k_f \delta_{12}) & \text{for } \dot{\delta}_{12} > 0 \\ \sin(-k_f \delta_{12}) & \text{for } \dot{\delta}_{12} < 0. \end{cases} \quad (5-5)$$

The $k_f = \pi$ is again kept constant. Now, Eq. (5-5) is equivalent to applying impulsive torques depending on the magnitude of the angular phase, δ_{12} , and the variation of the angular phase, $\dot{\delta}_{12}$.

Moreover, the influence of the W_{r_2} on the relative kinetic and potential energies is depicted in Figure 5.6(a)-(b), respectively, over time. Comparing the



(a)



(b)

Figure 5.5: Influence of the mitigation strategy (a) on the relative kinetic energies over time, (b) on the potential energies over time for $N_1 = 10.0$ N, $N_2 = 5.0$ N, and $\omega_{ref} = 2.5$ rad/s. The mitigation strategy is applied at $t = 100$ s and removed at $t = 150$ s.

energy magnitudes, one may notice that the W_{r_2} provides *acceptable* values of work via torque T_{r_2} with $N_2 = N_1/10$. Reminding Section 1.1.2 which describes the stick-slip phenomenon as energy transfer between potential and kinetic energies, this resistive torque T_{r_2} given by Eq. (5-5) prevents the increase of kinetic energy E_{k_1} by controlling the potential energies E_{p_1} and E_{p_2} . Therewith, it acts as an energy transfer control from potential energy to kinetic energy. Figure 5.6(a) depicts the relative kinetic energies of disc R_1 and R_2 , and the friction work at R_2 , while Figure 5.6(b) illustrates the potential energies and the friction work at R_2 . The latter figure shows the behavior of the second mitigation strategy proposal: if δ_{12} tends to increase, the T_{r_2} prevents it; if δ_{12} tends to decrease, the T_{r_2} also prevents it; if $\delta_{12} = 0$, $T_{r_2} = 0$. Meanwhile, the potential energy stored in k_2 spring decreases by the actuation of mitigation strategy. Thereby, the energy that would be transferred to accelerate R_1 is then extracted. In other words, the resistive torque represented by Eq. (5-5) avoids large values of δ_{12} .

Following, Figure 5.7 illustrates the mitigation of the vibration amplitudes of $\dot{\theta}_1$ and $\dot{\theta}_2$ over time. The stick-slip phenomenon is observed occurring on Disc 1, as shown in Figure 5.7(a). Thereafter at time $t = 100$ s, the mitigation is applied: one may note that the vibration amplitudes quickly decrease. Afterwards, at time $t = 150$ s, the mitigation strategy is turned off. Although Disc 2 (R_2) does not present stick-slip phenomenon, the torsional vibration amplitudes seen in Figure 5.7(b) also decreases. Further, the system remains in an equilibrium solution for $t > 150$ s.

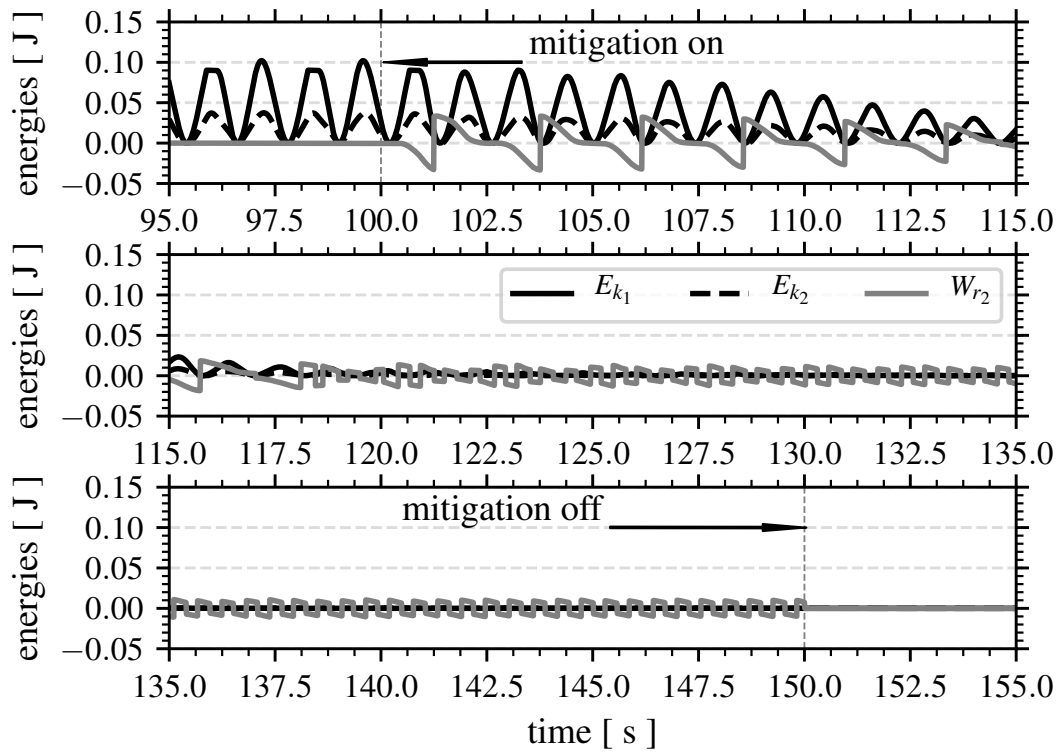
5.2

Experimental results

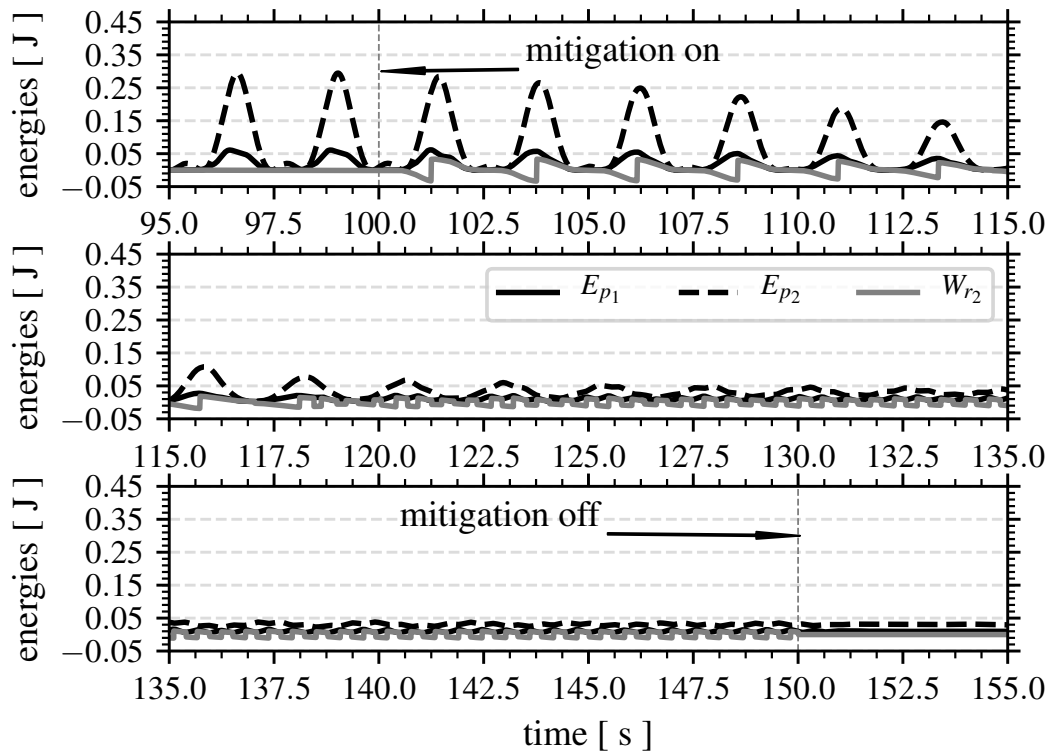
Herein, the device described in Chapter 3 is used. The servo controller is driven by an Arduino UNO board and then a sinusoidal signal is applied. At present, it is not possible to reproduce completely the proposed strategies on the drill-string experimental set-up, as described in previous section. However, the strategy experimentally possible to achieve is to induce friction torques only in one direction such as in Section 5.1.1

$$T_{r_2} = N_2 r_2 \mu_s \sin(\pi \delta_{12}). \quad (5-6)$$

Two reference angular velocities were tested: $\omega_{ref} = 2.0$ rad/s and $\omega_{ref} = 2.5$ rad/s. This values are in the bi-stability range (see Figure 4.12). One may observe in Figure 5.8 the peaks of the N_2 : the amplitude of the peaks are bigger than the expected value with $\omega_{ref} = 2.0$ rad/s. The influence of the application of the torque from Eq. (5-6) is very pronounced on $\dot{\theta}_2$. Also



(a)



(b)

Figure 5.6: Influence of the mitigation strategy (a) on the kinetic energies over time, (b) on the potential energies over time for $N_1 = 10.0$ N, $N_2 = 1.0$ N, and $\omega_{ref} = 2.5$ rad/s. The mitigation strategy is applied at $t = 100$ s and removed at $t = 150$ s.

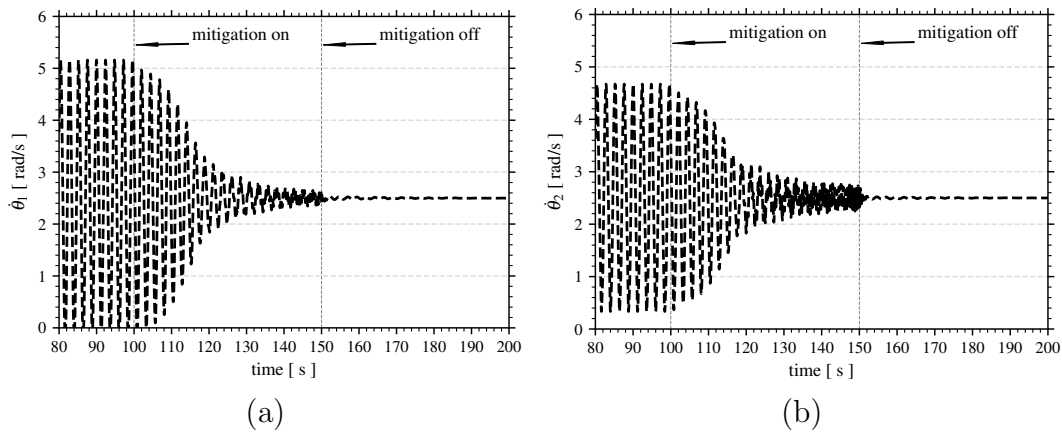


Figure 5.7: Influence of the mitigation strategy (a) on $\dot{\theta}_1$ and (b) on $\dot{\theta}_2$. $N_1 = 10.0$ N, $N_2 = 1.0$ N, and $\omega_{ref} = 2.5$ rad/s.

the stick time of the angular velocity $\dot{\theta}_1$ is reduced. Nonetheless after removing the torque provided by Eq. (5-6), the system returns to the stick-slip behavior. Figure 5.9 illustrates the behavior of the system with $\omega_{ref} = 2.5$ rad/s.

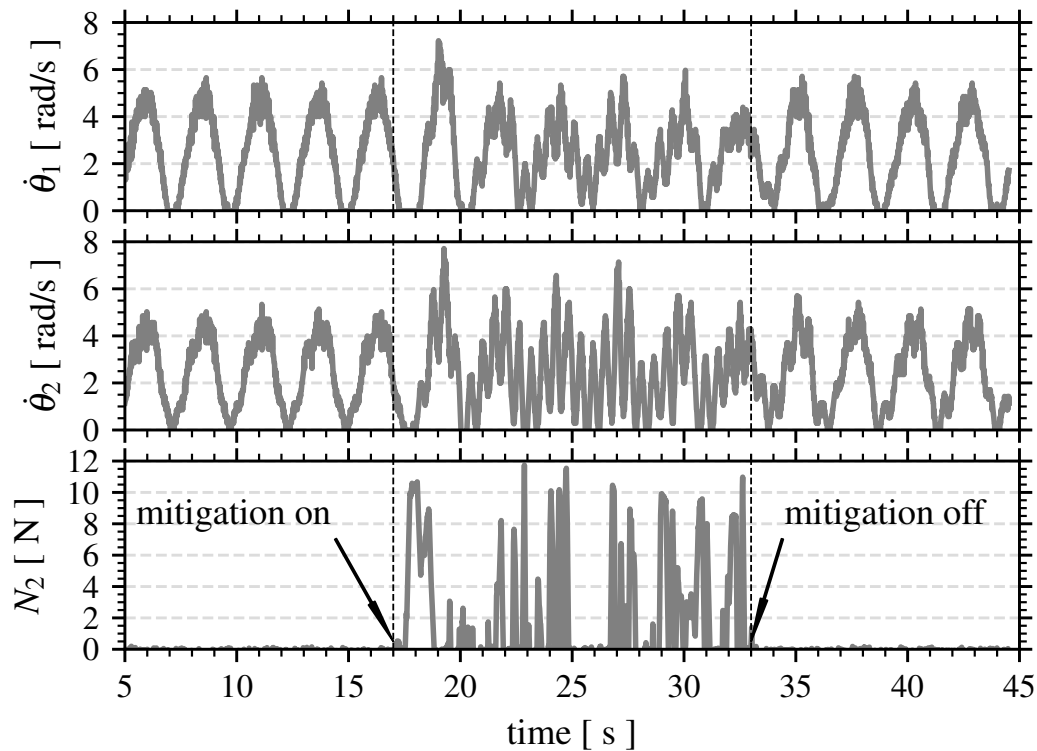


Figure 5.8: Influence of the mitigation strategy on the $\dot{\theta}_1$, $\dot{\theta}_2$, and N_2 application. $N_1 = 10$ N and $\omega_{ref} = 2.0$ rad/s.

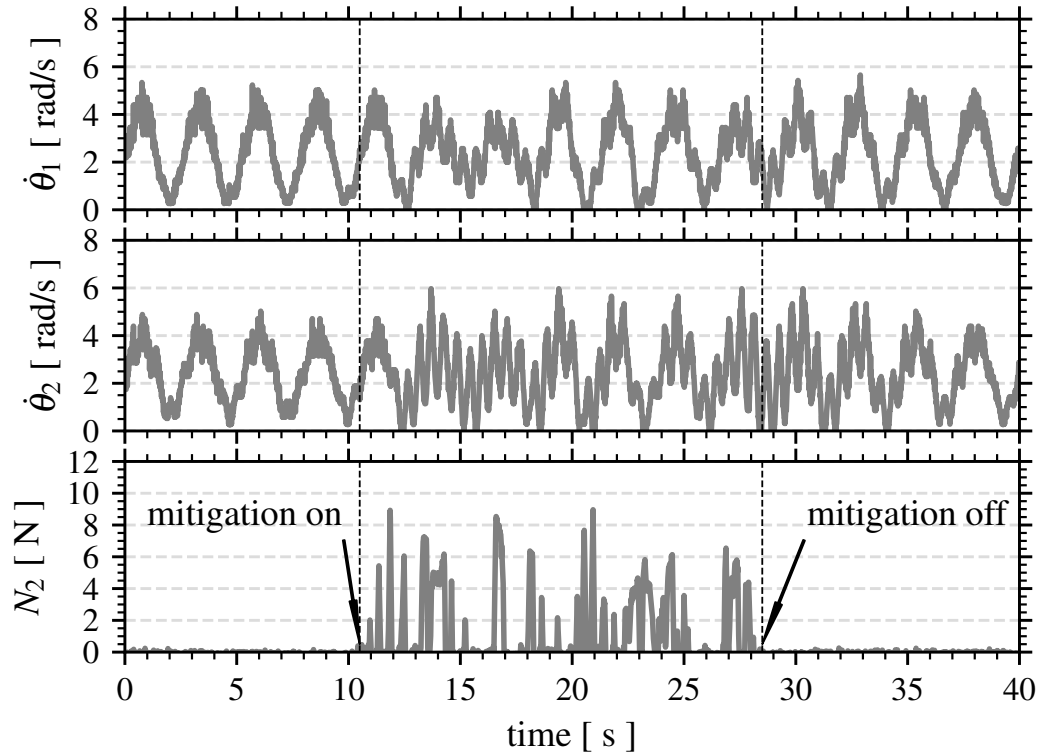


Figure 5.9: Influence of the mitigation strategy on the $\dot{\theta}_1$, $\dot{\theta}_2$, and N_2 application. $N_1 = 10$ N and $\omega_{ref} = 2.5$ rad/s.

5.3

Summary

This chapter is focused on the mitigation strategy to prevent stick-slip phenomenon. Besides the provided energy interpretation, one may also ascertain that the mitigation strategy of torsional vibration herein proposed consists of a control of bifurcations [105]. According to this reference, the methods for control of bifurcations commonly present the purpose of shifting bifurcation points, suppressing the bifurcation in a sequence, change the bifurcation nature, and/or change the character of a bifurcation set.

From this, the presented numerical results show a changing of the solution set, since the system performed a stable limit cycle and proceeded to present a stable equilibrium solution. These results proved that a friction torque acting on R_2 may provide the *sufficient* perturbation to change the solution of the system. It also presents *acceptable* values of work via friction (and $N_2 = N_1/10$) comparing to the relative kinetic and potential energies during stick-slip phenomenon. In fact, it must also be investigated in order to assume the minimum value possible. Recalling Section 1.1.2, the standard procedures to suppress the stick-slip phenomenon such as: increase the Surface RPM, and decrease the weight-on-bit. It should be remarked that the combination of N_1

and ω_{ref} (representing weight-on-bit and Surface RPM, respectively, in field operation) was not modified to mitigation purpose.

In the section of the experimental results, only one strategy proposed in Section 5.1 was conducted: the first mitigation strategy. By using the pin and the servo controller it was only possible to impose a torque against the rotation direction. Thereby, one noticed the T_{r_2} may control the energy transfer to the Disc 1 (R_1) presenting a reduction of the stick time, but not a complete mitigation of torsional oscillations. Thereafter the removal of the T_{r_2} , the system returns to the stable limit cycle (torsional vibration). Furthermore, the delay and the frequency of the servo controller actuation were not considered in numerical simulations which may have great influence on the final result. For the second strategy, an embedded DC-motor on R_2 is already installed [42]. However, the implementation of this second mitigation strategy is being developed for acquisition of the experimental results.

It is worth mentioning that there are normal force limitations in order to prevent damage to experimental set-up components such as servo controller, load cells, shaft and DC-motor.